International Journal of Concrete Structures and Materials

RESEARCH Open Access

The Mechanical Properties of Alkali-Activated Slag-Silica Fume Cement Pastes by Mixing Method

Taewan Kim[1] and Choonghyun Kang[2*]

Abstract

The mixing method is the investigation of the characteristics of alkali-activated cement paste (AACP) with slag and silica fume (SF) of 1: 1. The basic mixing method is ASTM C305, which is defined as 1st-cycle. There are three factors considered in this experiment; (i) the addition of mixing time (2nd-cycle), (ii) the concentration of activator depending on the amount of mixing water, and (iii) the mixing sequence of slag and SF. It was found that the second cycle, the additional mixing time, had the effect of improving the mechanical properties. In addition, accelerated activation through the mixing of slag with a high concentration of alkali solution in the 1st-cycle increases the hydration products and decreases the porosity and increases the mechanical properties. Therefore, it was found that the change of the mixing method in the AACP composed of slag and SF 1: 1 has a great influence on the mechanical properties. As a result, the method of first mixing slag in aqueous solution of high alkali concentration in AASC mixed with slag and SF improves the mechanical properties.

Keywords: mixing method, mixing time, mixing sequence, mechanical properties

1 Introduction

Alkali-activated slag cement (AASC), which used ground granulated blast-furnace slag (slag) as its main binder as well as an alkali activator, is attracting attention as an eco-friendly cement. Many researchers have published various studies on AASC (Provis et al. 2015; Rashad 2013; Bernal and Provis 2014; Burciaga-Díaz and Escalante-García 2013). A number of admixtures are used together with slag, including fly ash (FA), silica fume (SF), and metakaolin (MK). Studies on the mechanical properties and microstructure of AASC mixed with these admixtures are ongoing (Alanazi et al. 2019; Gülşan et al. 2019; Zhang et al. 2020).

Silica fume (SF) has long been used as a cement admixture. Silica fumes are amorphous oxides (SiO_2), generated as industrial byproducts during production of ferrosilicon and the like. SF is amorphous, which comprises the majority of the constituents, and exhibits a fine spherical shape with a diameter of 1 μm or less. These silica fumes were found to be effective in enhancing the strength, chemical resistance, and durability of concrete through the pozzolanic reaction and formation of reaction products with Si when it is used as an admixture of cement.

Several studies on SF have been performed based on AASC. Rostami and Behafarnia (2017) investigated the effects of curing conditions on alkali-activated slag concrete substituted with SF by 5, 10, and 15% slag mass. As a result, it was reported that water curing is a method of increasing compressive strength and decreasing permeability. Collins and Sanjayan (1999) investigated the properties of condensed silica-fume (CSF) and ultra-fine slag (UFS) influencing workability and strength development in alkali-activated slag concrete (AAS). The 10% CSF announced the trend of high demand for water and minimal loss of workability of UFS. Rashad and Khalil (2013)

*Correspondence: chkang@gnu.ac.kr
[2] Department of Ocean Civil Engineering, Gyeongsang National University, Tongyeong 53064, Republic of Korea
Full list of author information is available at the end of the article
Journal information: ISSN 1976-0485 / eISSN 2234-1315

Springer Open

© The Author(s) 2020. This article is licensed under a Creative Commons Attribution 4.0 International License, which permits use, sharing, adaptation, distribution and reproduction in any medium or format, as long as you give appropriate credit to the original author(s) and the source, provide a link to the Creative Commons licence, and indicate if changes were made. The images or other third party material in this article are included in the article's Creative Commons licence, unless indicated otherwise in a credit line to the material. If material is not included in the article's Creative Commons licence and your intended use is not permitted by statutory regulation or exceeds the permitted use, you will need to obtain permission directly from the copyright holder. To view a copy of this licence, visit http://creativecommons.org/licenses/by/4.0/.

reported experimental results on the elevated-temperature performance in alkali-activated slag cement (AASC) paste substituted with SF by 0, 5, 10, and 15%. At four exposure temperatures of 400, 600, 800, and 1000 °C, AASC, including SF, is more resistant to sudden thermal shock in high temperature environments. Aydin (2013) studied the properties of binary and ternary combination cement mortars mixed with slag, fly ash, and SF. The SF was substituted by 0, 10, 20% of the binder weight. Experiments consisted of the compressive strength, flexural strength, water absorptivity, permeable voids, and drying shrinkage. As a result, an optimal AAC composition was obtained with ternary blended cement containing 20.3% FA, 18.9% SF and 60.8% GGBFS. Li et al. (2014) reported the temperature effect of SF on AASC paste. The SF substituted 5, 15, and 50% by weight of slag. As a result of the experiment, partial replacement of slag with SF significantly reduced the strength loss, and it was reported that 50% slag + 50% SF samples did not show strength loss under curing conditions at 25 and 60 °C.

Gao et al. (2015) reported that the slump flow decreased significantly with increasing the nano-silica content in alkali-activated slag-fly ash blends cement pastes. The slag/fly ash ratios are 70/30 and 30/70, and nano-silica is 0, 1, 2, and 3% of the binder mass. Aydin and Baradan (2013) studied the mechanical properties and drying shrinkage behavior for steel fiber reinforced alkali-activated slag/silica fume (AASS) mortars. The SF substituted 20% of slag mass. As a result, it was mentioned that AASS mixed with steel fiber showed high mechanical performance and reduced shrinkage.

However, SF has a high specific surface area because of its fine particle size, which means that a large amount of mixing water is required (Nochaiya et al. 2010). Otherwise, a large amount of superplasticizer should be used to ensure fluidity. The fine particles of SF are inhomogeneously dispersed when the mixing water or superplasticizer is insufficient, thereby deteriorating the mixture's performance (Diamond and Sahu 2006).

The SF has lower hydration performance than OPC, slag, and fly ash. Thus, previous studies have suggested that SF has the largest filler effect than nucleation effect and pozzolanic reaction. In alkali-activated slag cement, SF is less activated by alkali activator than slag. Therefore, it is expected that it is possible to control the mechanical properties by using the difference in activation ability of slag and SF in AASC. As a method of controlling these mechanical properties, approaches to mixing methods have been rare. There have been studies in which 3, 10, and 30 min mixing times were added for slag paste and mortars activated by waterglass (Palacios and Puertas 2011). It has been reported that specimens with an additional 30 min of mixing time increase the compressive strength and decrease the porosity. However, studies on the mixing method of AASC other than Palacios and Puertas (2011) are difficult to find.

The purpose of this study is to investigate the mechanical properties of alkali-activated cement paste composed of 1: 1 slag-silica fume by mixing method. The mixing ratio of slag and SF was determined to be 50%: 50% in order to exclude the effect of the slag or SF substitution ratio. It is difficult to clearly know the effect of SF because the effect of hydration of slag is large when the SF having little reactivity with the alkali activator is mixed in a proportion less than 50%. Conversely, when the SF exceeds 50%, the amount of slag decreases relatively, resulting in a sharp decrease in the mechanical properties and a problem of heterogeneous dispersion of SF. Therefore, in order to confirm the effect by the mixing method most clearly, it was decided to be 50%: 50%, which can ignore the effect of the mixing ratio of slag and SF.

Numerous research reports on alkali-activated cement (AAC) have indicated that the type, concentration, nature of binder, type and amount of admixture, and curing temperature affect the mechanical properties (Awoyera et al. 2019; Awoyera and Adesina 2019; Sun et al. 2020; Zhang et al. 2020). Particularly, when silica-fume or fly-ash, etc. having low hydration by an alkali activator is included (or substituted) in the binder, the mechanical properties are reduced. For this, a method of increasing the concentration of the activator or increasing the curing temperature is used. The purpose of this study was to develop a method to improve the mechanical properties without increasing the amount of activator used and without the high temperature curing process. Among various methods that can be tried, an attempt was made to improve the mechanical performance through a mixing method that increases the mixing time, the order of injection of the binder, and the amount of activation.

Table 1 The properties of slag and silica fume.

	Chemical components (%)								Density (g/cm^3)	Fineness (m^2/kg)	LOI (%)
	SiO_2	Al_2O	Fe_2O	MgO	CaO	K_2O	SO_3	Na_2O			
Slag	35.30	12.58	0.79	3.19	41.30	0.63	4.75	0.33	2.84	420	0.32
Silica fume	94.24	0.57	1.33	0.42	1.51	–	–	–	2.28	22,000	0.84

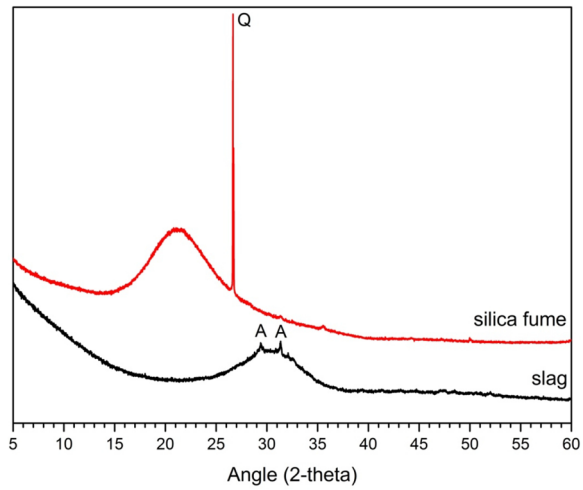

Fig. 1 XRF of slag and silica fume, *Q* quartz, *A* akermanite.

2 Materials and Experiments

2.1 Materials

The chemical compositions of silica fume (denoted by SF) and ground granulated blast furnace slag (denoted by slag) used in this study are presented in Table 1 as obtained through XRF analysis. And SF used in the experiment is a product sold by Elkem, and slag is a KRT product in Korea. Figure 1 shows the results of X-ray diffraction (XRD) analysis. The XRD analysis of the silica fume shown in Fig. 1 shows a hump between 15 and 27°. This hump means that most of the constituents of SF are composed of SiO_2 of amorphous phase. An XRD of the slag also finds an amorphous hump between 25 and 35°.

The activator agents used in the experiment were NaOH (sodium hydroxide, purity ≥ 98%, pellet type, SAMCHUN chemical) and Na_2SiO_3 (sodium silicate, Ms = 2.0, liquid type, SAMCHUN chemical). The concentration of the activator was 5 wt % NaOH + 5 wt % Na_2SiO_3 by weight of binder (13.8 M NaOH and 4.5 M Na_2SiO_3); these compounds were incorporated into the mixing water prior to mixing and were allowed to stand in the laboratory for 6 h before use (a mixture of mixing water and 5wt % NaOH + 5wt % Na_2SiO_3 is referred to as an aqueous solution).

2.2 Experiments

The mixing ratio of slag: SF was 1:1 by weight, and the water-binder ratio (w/b) was 0.55 considering the consistency due to mixing of SF. The w/b was selected to be 120 ± 10 mm in flow value without using superplasticizer in consideration of plasticity and workability. This w/b value is for the slag + SF mixture and was determined by preliminary experiments prior to the main experiment. The slag + SF mixture is paste. To perform a comparison of the mixing methods and strength characteristics obtained by SF, a control sample of 100% slag was prepared using the same w/b ratio and activator concentration for comparison.

This study focuses on the fact that slag is faster and more active than SF at the same alkali concentration and mixing conditions when considering mixing method. The change factors of the mixing method considered in this study are as follows. (i) Addition of the same mixing time. The added time is indicated by 2nd-cycle (10S-T, 5S5F-T, 5S5F-TA, 5S5F-TB), (ii) Control of the amount of activator: total activator use (5S5F-TA), half activator use (5S5F-TB). The factors considered are compared with 10S, the basic mixing method using 100% slag, and 5S5F, the basic mixing method with 50% slag + 50% SF. This study examines the reactivity difference and mechanical properties of slag-SF according to the change of mixing method considering these three conditions.

Since this study focuses on the strength characteristics of the combination of SF and slag, the mixing method is as follows. The basic mixing method and time are based on those of ASTM C305. The standard method used is for ordinary Portland cement, but the application to the AASC of this study was due to the determination that the mixing procedure could be appropriate to obtain a homogeneous paste. All the orders are observed to remain the same; however, after slow speed (140 ± 5 r/min, 30 s), the stopping time increases from standard 15 s to 30 s. This is to facilitate the scrape of the paste. The methods employed for each mixture are as follows.

The 10S method mixes 100% slag with an alkaline activated aqueous solution at low speed (140 ± 5 r/min) for 30 s. Then stop mixing for 30 s and scratch the paste on the wall of the mixing bowl. Mixing for the next 30 s is made at medium speed (285 ± 10 r/min), after which it stops again for 90 s. Finally blend at medium speed for 60 s. The total mixing time is 270 s. This is a procedure and time similar to ASTM C305 and defined as 1st-cycle. The 10S-T method is mixed in the same way as 10S method, but an additional 270 s cycle is added (2nd-cycle) without additional material input.

The 5S5F method is made of slag + SF in an aqueous solution containing the mixing water and the activating agent, mixed in the same cycle used for 10S method. 5S5F method and 10S method require 270 s of mixing time. The 5S5F-T method is mixed in the same manner as 5S5F method, but again, the 2nd-cycle is added. The total mixing times of 5S5F-T and 10S-T take 540 s.

The 5S5F-TA method is created by placing slag in an aqueous solution containing only half of the mixing water and activating agent, as used for 5S5F method, and was then mixed during the 1st-cycle. Then mixing SF with the remaining half of the mixing water and activator. Further,

it is mixed during the 2nd-cycle. The 5S5F-TB method is formed in the same way as 5S5F-TA method, except that it uses the full amount of the activator during the 1st-cycle. Since both 5S5F-TA and 5S5F-TB methods are combined in the 2nd-cycles, it takes 540 s to complete mixing.

Each mixing method represents a variation of the mixing time, the order of introduction of the ingredients, the starting point, the concentration of the activator, and the like (see Table 2).

After mixing according to each method, samples were placed in a mold and stored in a constant-temperature, constant-humidity chamber (RH 90 ± 5% and 23 ± 2 °C) for 24 h. All molds of the samples were then removed and the samples stored in a constant-temperature, constant-humidity chamber (RH 90 ± 5% and 23 ± 2 °C) until the measurement time.

The compressive strength was 25 × 25 × 25 mm cubic shape, measured according to ASTM C109, and the average value of three samples was used.

The compressive strength was in accordance with the procedure of ASTM C109, and a cube-shaped specimen measuring 25 × 25 × 25 mm was used. Compressive strength is the average of the values measured for three samples. Strength measurements were performed at 1, 7, and 28 days. Experiments for analysis of microstructure and pore characteristics are summarized in Table 3. The XRD and SEM/BSE samples are immersed in acetone for 12 h and then dried in a vacuum desiccator for 48 h. The hydration stopped samples were subjected to a pulverization process to measure XRD. The SEM/BSE samples were polished with SiC grinding disks followed by platinum coating.

Ultrasonic pulse velocity (UPV) was measured using a prismatic bar of 40 × 40 × 160 mm. For the first measurement, install the receiver on the right side and install the transmitter on the left side to read the UPV value. Then re-measure the UPV by changing the position of the receiver and transmitter (transmitter on the right, receiver on the left). In this way, the average of the measured values by changing the position of the receiver and the transmitter is taken as one measurement value. The UPV is the average of the measurements for the three prismatic bars.

This study confirms the effect of the new mixing method on the activation of slag-silica fume. Other analyzes used samples from 1 and 28 days. However, SEM/BSE only used samples from 1 day. SEM/BSE attempted to analyze the microstructure for ages with the greatest variability of strength based on the results of compressive strength experiments. The purpose of this study was to find and analyze the cause of the greatest intensity change through the analysis of the microstructure. Therefore, the compressive strength variability at 1 day was the highest and was selected as the SEM/BSE analysis sample.

The number of 25 × 25 × 25 mm cubic samples in each mixing method is 12 EA. The quantity used for compressive strength measurement was 9 EA (at 1, 7, and 28 days × 3 EA), 1EA for SEM/BSE observation, and 2 EA for mercury-intrusion porosimetry (MIP) measurement. In addition, 3 EA samples of 40 × 40 × 160 mm used for ultrasonic pulse velocity (UPV) measurement were prepared.

3 Results and Discussion

3.1 Compressive Strength

Figure 2 shows the compressive strength results for each mixing method. SF mixing improved the compressive strength. This is consistent with previous studies that reported the improvement in compressive strength in alkali-activated cement using SF (Alanazi et al. 2019; Cheah et al. 2019; Gülşan et al. 2019; Wetzal and Mddendorf 2019; Ramezanianpour and Moeini 2018). SF promotes the filler effect of pore filling and the formation of C-S–H gel, which is a hydration product, contributing to the improvement of compressive strength by forming a dense matrix (Rostami and Behafarnia 2017; Rashad and Khalil 2013; Behfarnia and Rostami 2017). In a study by Palacios and Puters (2011), waterglass activated slag pastes and mortars reported an increase in compressive strength as mixing time increased to 3, 10 and 30 min. In the results of this study, the additional mixing time by 2nd-cycle shows similar results to improve the compressive strength.

The 10S-T and the 5S5F-T methods increased the compressive strength at all measurement days as the mixing time increased due to the addition of 2nd-cycle. These results can be clearly seen by comparing the compressive strengths of 10S and 5S5F method with 10S-T and 5S5F-T as shown in Fig. 2. Therefore, the increase of mixing time has the effect of improving the compressive strength in AASC regardless of the with or without of SF. The reasons for the increase in compressive strength by the mixing method can be considered as the following two. First, increasing the mixing time by 2nd-cycle increases the contact area and time between the activator and slag particles. This has the effect of promoting the hydration of more slag particles. The second is to increase the formation of hydration reactants due to the nucleation effect of the slag particles in which SF is activated, and to form a dense matrix by the filler effect.

The newly applied mixing methods 5S5F-TA and 5S5F-TB methods are compared with 5S5F and 5S5F-T methods. The compressive strength of specimens with 5S5F-TA method was similar to that of 5S5F-T method. However, the 5S5F-TB method showed higher

Table 2 Mixing methods and procedures of paste.

	10S	5S5F	10S-T	5S5F-T	5S5F-TA	5S5F-TB
Ready	Place all the mixing liquid (total water + total activator) in the bowl				Place all the mixing liquid (water/2 + activator/2) in the bowl	Place all the mixing liquid (water/2 + total activator) in the bowl
1st-cycle	Add the 100% slag in the bowl and allow 30 s for the absorption of the liquid	Add the binder (slag + SF) in the bowl and allow 30 s for the absorption of the liquid	Add the 100% slag in the bowl and allow 30 s for the absorption of the liquid	Add the binder (slag + SF) in the bowl and allow 30 s for the absorption of the liquid	Add the slag in the bowl and allow 30 s for the absorption of the liquid	
	Start the mixer and mix at the slow speed (140 ± 5 r/min) for 30 s					
	Stop the mixer for 30 s and during this time scrape down into the batch any paste that may have collected on sides of the bowl					
	Start the mixer and mix at the medium speed (285 ± 10 r/min) for 30 s					
	Stop the mixer and let the paste stand for 90 s. During the first 15 s of this interval, quickly scrape down into the batch any paste that may have collected on the side of the bowl; then for the remainder of this interval, close the mixer enclosure or cover the bowl with the lid					
	Finish by mixing for 60 s at medium speed (285 ± 10 r/min)					
2nd-cycle			Stop for 30 s		Add the SF and liquid (water/2 + activator/2) in the bowl for 30 s	Add the SF and water/2 in the bowl for 30 s
			Start the mixer and mix at the slow speed (140 ± 5 r/min) for 30 s			
			Stop the mixer for 30 s and during this time scrape down into the batch any paste that may have collected on sides of the bowl			
			Start the mixer and mix at the medium speed (285 ± 10 r/min) for 30 s			
			Stop the mixer and let the paste stand for 90 s. During the first 15 s of this interval, quickly scrape down into the batch any paste that may have collected on the side of the bowl; then for the remainder of this interval, close the mixer enclosure or cover the bowl with the lid			
			Finish by mixing for 60 s at medium speed (285 ± 10 r/min)			

Table 3 Summary of experiments.

Test	Equipment	Measurement day (day)	Conditions
Pore structure (mercury-intrusion porosimetry; MIP)	AutoPore IV9500, Micromerities	1, 28	Surface tension : 485 dyn/cm, mercury (Hg) density : 13.534 g/mL
Hydration products (X-ray diffraction; XRD)	Xpert3, PANalytical	1, 28	5–60° (2θ), Cu-K radiation (k = 1.54443 Å), step size : 0.017 (2 θ)
Thermal analysis (DSC)	SDT Q600, TA Instruments	1, 28	30–800 °C, 20 °C/min, N_2 gas environment
Ultrasonic pulse velocity (UPV)	CCT-4, Proceq	1, 28	Prismatic bar (40 × 40 × 160 mm)
Microstructure observation (scanning electron microscope/back-scattered electron images; SEM/BSE)	SUPRA 40, Zeiss	1	Accelerating voltage : 15 kV, the high vacuum mode, energy dispersive spectroscopy (EDS)

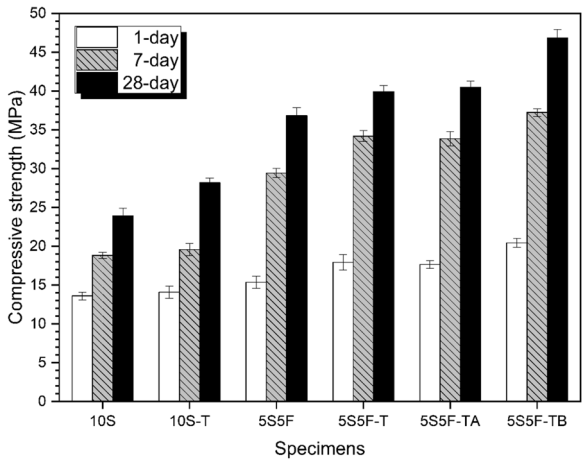

Fig. 2 Compressive strength according to each mixing method.

compressive strength values than 5S5F method and 5S5F-T method, and it was the highest among all mixing methods.

The maximum compressive strength of 5S5F-TB method was due to the reaction of slag with a high concentration of alkaline aqueous solution produced by half of the mixing-water and the total activator. This reaction induces the rapid activation of slag in the early stage of hydration, eluting many ions and forming a hydration reactant. As a result, SF is properly dispersed in the 2nd cycle in the state where the slag activation reaction is maximized, and the filler effect and the nucleation effect generate synergistic effects, forming a dense matrix. This results in an improvement in compressive strength.

Table 4 shows the compressive strength values of 5S5F-T, 5S5F-TA, and 5S5F-TB methods for the 5S5F method to calculate the rate of change of compressive strength according to the mixing method.

Table 4 Compressive strength change rates (%).

Age (day)	5S5F-T/5S5F	5S5F-TA/5S5F	5S5F-TB/5S5F
1	116.6	114.9	133.0
7	108.8	115.0	126.5
28	105.5	109.9	127.2

In Table 4, the 5S5F-TB method showed the highest compressive strength growth rate for both 1, 7, and 28 days. 5S5F-T, 5S5F-TA, and 5S5F-TB methods showed higher 1 day compressive strength increase rate. This means that the initial strength of the compressive strength can be influenced by changing the mixing time, the order of slag-SF injection, and the concentration of activator in the initial hydration stage.

From Fig. 2 and Table 4, the compressive strength was improved only by the variation of the mixing method. This confirms that it is possible to increase the compressive strength without additional admixture, superplasticizer, high concentration of activator, and high-temperature curing.

This increase in compressive strength is evident in the 5S5F-TB method. The 5S5F-TB method is considered to be effective in improving the compressive strength. First, the slag was injected in the 1st-cycle to induce sufficient hydration reaction. Second, a total-activator was used for the 1st-cycle in half mixing-water. This activator formulation dramatically enhances the hydration of slag by creating a highly alkaline aqueous solution environment. These two actions promote the formation of slag hydration products, and the nucleation and filler effect of SF contributes to forming a dense matrix, which increases the compressive strength.

Relatively, the 5S5F-TA method is the same as the 5S5F-TB method in which the slag is preferentially applied in the 1st-cycle. However, the use of half-mixing-water and half-activators has lower slag activation than the 5S5F-TB method. However, the compressive strength of the 5S5F-TA method is higher than that of the 5S5F method and is similar to that of the 5S5F-T method. As a result, it was confirmed that using the total-activator for the 1st-cycle in half mixing-water is more effective for increasing the compressive strength. This is consistent with the previous reports of AASC that compressive strength increases with increasing activator concentration.

3.2 Hydration products

Figure 3 shows the results of the analysis of the hydration products by each mixing method. In Fig. 3, the main hydration products are C-S–H gel. Also, hydration products were observed differently depending on the presence or absence of SF substitution. Figure 3a shows the results of hydration products analysis at 1 day. Monosulfate, hydraotalcite, and akermanite were found in the 10S and 10S-T methods without SF substitution. However, 5S5F, 5S5F-T, 5S5F-TA, and 5S5F-TB methods substituted with SF showed almost no hydration products other than C-S–H. The tendency of these hydration products is similarly observed at 28 days shown in Fig. 3b.

In Fig. 3a, b, specimens with SF replaced showed gentle hump in the region of 15–25°. This is similar to the amorphous hump form of SF shown in Fig. 1. Therefore, in the XRD of SF, an amorphous hump in the 15–25° region is observed. This is clearly seen when compared to the 15–25° region of the 10S and 10S-T methods that do not replace SF. The amorphous hump in the 25–35° region observed in Fig. 3a, b was similar in 5S5F, 5S5F-T, 5S5F-TA, and 5S5F-TB methods without significant change. Similarly, the 10S and 10S-T methods showed similar trends with little change in the hump in the 25–35° region. The mixing method proposed in this study hardly changed the peak size and amorphous hump morphology of the major hydration reactants. Thus, mixing method has a minimal effect on the change of hydration reactants. In other respects, it can be inferred that there are other causes that can more clearly explain the tendency of strength with mixing method.

At 1 day and at 28 days, the 10S and 10S-T methods showed a slightly higher CSH peak than the other mixing methods. The 10S and 10S-T methods is a 100% slag binder and the other mixing method is a binder consisting of 50% slag and 50% SF. Thus, as expected, the reduction in the amount of slag also reduces some of the hydration products. 5S5F and 5S5F-T of "50% slag + 50% SF" have 50% less amount of slag compared to 10S and 10S-T using 100% slag. In a previous study, the main

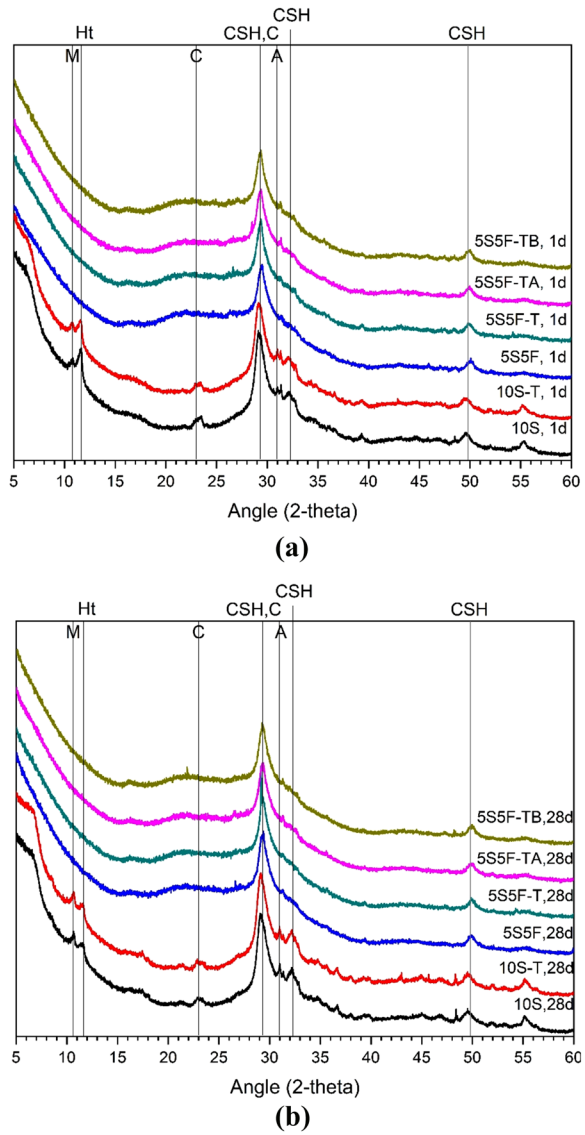

Fig. 3 XRD results by hydration products analysis, **a** 1 day, **b** 28 days, *M* monosulfate, *Ht* hydrotalcite, *C* calcite, *A* akermanite, *CSH*: C-S–H.

hydration reactant of alkali-activated slag cement was reported to be C-S–H. Therefore, when the amount of slag decreases, the amount of C-S–H produced by reaction with the activator also decreases. This reduction in hydration reactants acts as a cause of reduction in mechanical performance. However, the fine particles of SF have an effect of promoting nucleation in the step of forming a hydration reactant during the activation reaction of slag. In addition, SF particles compensate for the deterioration of mechanical performance by forming hydration reactants into a dense microstructure due to filler effect. In some studies, SF is reported to promote

the formation of C-S–H gel in alkali-activated cement (Rashad and Khalil 2013; Rossen et al. 2015; Berodier and Scrivener 2014). In the scope of this study, no clear change was observed as a result of comparing the sizes of C-S–H gel peaks according to the mixing method. However, in the XRD analysis, it is unclear to evaluate the amorphous C-S–H gel. In addition, the analysis is not clear due to the overlap of calcite and C-S–H gel peaks. The analysis of the hydration product will be reviewed later in the thermal analysis.

3.3 Pore Structures

Figure 4 shows the MIP results for at 1 day and at 28 days for each mixing method. All mixing methods showed a decrease in the size of pores at 28 days and 1 day. The pore size and volume of 50% slag + 50% SF sample were decreased compared to 100% slag sample (without SF). These results are consistent with previous studies on alkali-activated cement mixed with SF (Gao et al. 2015; Duan et al. 2013; Zhang and Li 2011; Wongkeo et al. 2012). The samples with similar pore size distribution at 1 day and 28 days are 10S-T and 5S5F-TB methods. The similarity of these pore size distributions appears when the mixing time is increased with the 100% slag binder (10S-T method). The 5S5F-TB method is the case where the slag is mixed with a high concentration of alkali solution (total activator + half mixing water) in the 1st-cycle. The two mixing methods mentioned can be attributed to the fact that the contact time and area of the slag and the activator are increased and the concentration of the activator is high, which promotes the hydration of the slag. Therefore, the mixing method has been shown to reduce the fluctuation of pore size by increasing the contact time and area of the slag particles with the activator in a highly alkaline environment.

Changes in the mixing method affect the change in pore distribution in the hydration products matrix, which can be inferred to have a significant effect on the strength of AAC. In particular, it was confirmed that it is possible to influence the pore structure without using the concentration of the activator or the high temperature curing method only by changing the mixing method.

Table 5 shows the total porosity and analysis of pore size for all mixing methods from MIP analysis. The pore sizes are classified in Mindess et al. (2003) and are classified into three types: large capillary pores (10–0.05 μm), medium capillary pores (0.05–0.01 μm) and gel pores (less than 0.01 μm). In Table 5, the total porosity of 5S5F method substituted with SF was lower than that of 10S method without SF. Previous studies have also concluded that substitution of SF reduces the porosity or pore size of AASC. In addition, the total porosity of 10S-T, 5S5F-T, 5S5F-TA, and 5S5F-TB methods, which added mixing time, also showed a tendency to decrease. In Table 5, the 5S5F-TB method shows the lowest total porosity at 1 day and 28 days. Despite the fact that the amount of slag decreased by half compared with 10S and 10S-T methods, the reason why the low total porosity was measured is two. The first is the void filling effect by the filler effects of SF. Second, in the 1st-cycle, activation of the slag by a high concentration of alkali solution (total activator + half mixing-water) promotes the formation of hydration products. These two effects work simultaneously to form a matrix of the 5S5F-TB method, and as a result, it can be assumed that the size and amount of pores decrease. The decrease in total porosity affects the increase in compressive strength. Therefore, as shown in the compressive strength results of Fig. 2, 5S5F-TB method has the highest compressive strength.

Table 5 shows the change in pore size distribution according to the mixing method. In the mixing method, the additional time (2nd-cycle) tends to decrease the amount of medium capillary pores and increase gel pores. This change in pore size contributes to the reduction of the total porosity by reducing the pores larger than the medium capillary pores. "5S5F" reduced large capillary pores and increased gel pores than the "10S" sample. This means that 50% slag + 50% SF forms a denser matrix than 100% slag, which can also be confirmed by a decrease in the total porosity value. In addition, the method of mixing slag in 1st-cycle and SF in 2nd-cycle further promotes slag activation to form a dense matrix, which reduces the size of pores. As a result, the gel pores of 5S5F-TA and 5S5F-TB show the largest values compared to other mixing methods at 1 day and 28 days. In addition, 5S5F-TB, which uses the activator all at 1st-cycle, shows higher gel pores than 5S5F-TA, which uses only half the activator at 1st-cycle. It can be seen that the high concentration of alkaline environment promotes the slag activation reaction, thereby reducing the size of the pores, thereby forming a more dense matrix. Therefore, it is considered that through the change of the mixing method, the size of the pores existing in the matrix is reduced, and the total porosity is also reduced, thereby densifying and contributing to the improvement of compressive strength.

3.4 Thermal Analysis

Figure 5 shows the thermal analysis results of the hydration products for each mixing method. Figure 5a shows DSC results for 1 day samples, and Fig. 5b shows an enlarged area smaller than 300 °C in Fig. 5a. Figure 5d shows the enlargement of the region below 300 degrees in Fig. 5c, which is the thermal analysis result for 28 days.

At 1 day and 28 days confirmed C-S–H in the 50–200 °C temperature range (Haha et al. 2011; Bakolas et al. 2006). C-S–H and calcite were observed in all

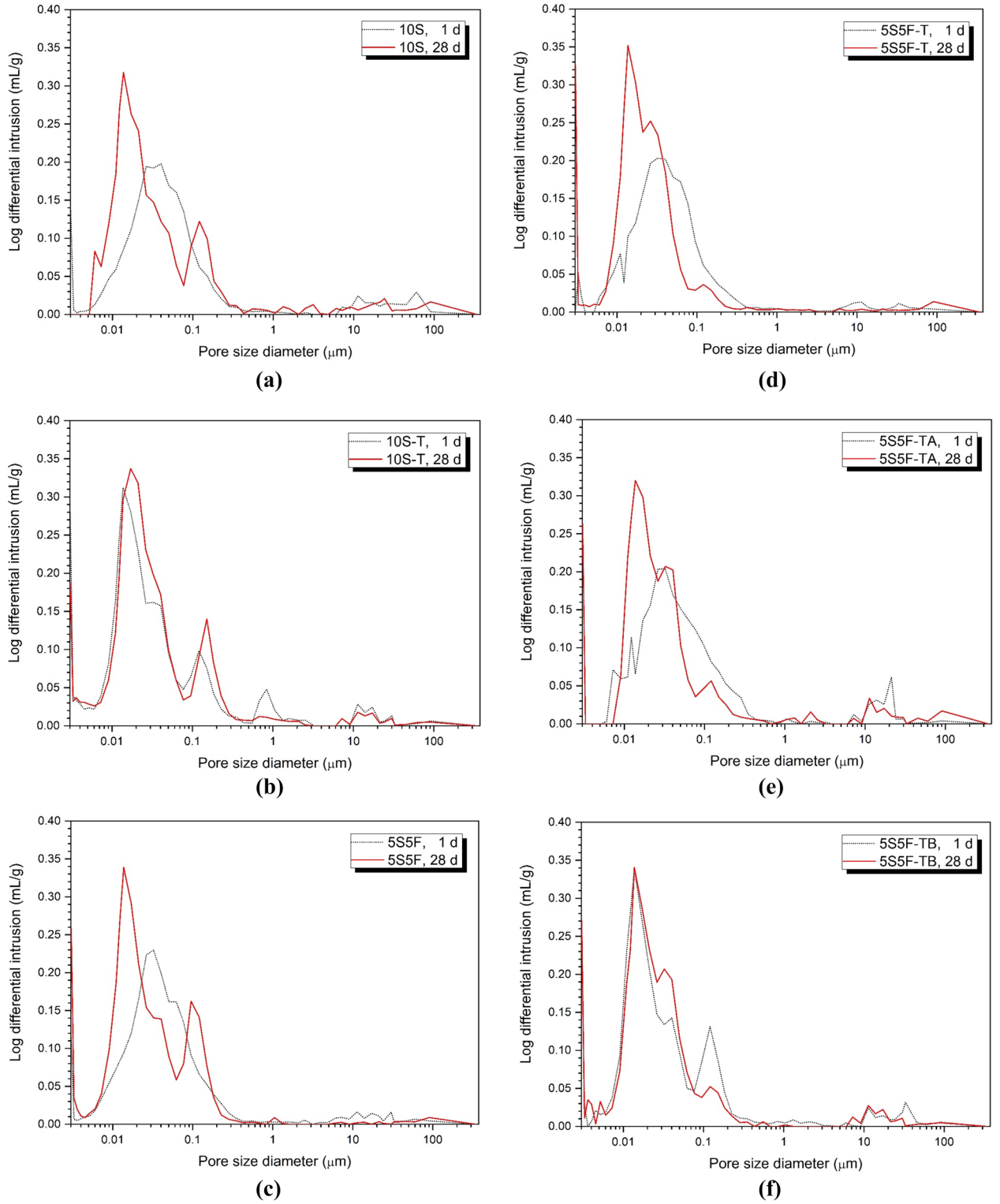

Fig. 4 Pore structure analysis at 1 day and 28 days, **a** 10S, **b** 10S-T, **c** 5S5F, **d** 5S5F-T, **e** 5S5F-TA, **f** 5S5F-TB.

Table 5 Analysis of total porosity and pore distribution according to mixing method (from MIP analysis).

	Age	10S	10S-T	5S5F	5S5F-T	5S5F-TA	5S5F-TB
Total porosity (%)	1 day	36.9	34.9	33.4	33.0	31.3	31.8
	28 days	35.8	33.3	33.7	32.1	31.5	30.8
Large capillary pores (10–0.05 μm) (%)	1 day	2.12	2.16	2.43	2.36	1.95	1.79
	28 days	1.98	2.35	1.94	1.53	1.79	0.88
Medium capillary pores (0.05–0.01 μm) (%)	1 day	86.89	83.77	86.05	86.57	82.68	82.08
	28 days	86.76	82.31	82.02	82.34	82.08	81.51
Gel pores (≤ 0.01 μm) (%)	1 day	10.99	14.07	11.52	11.07	15.37	16.13
	28 days	11.26	15.35	16.04	16.13	16.14	17.61

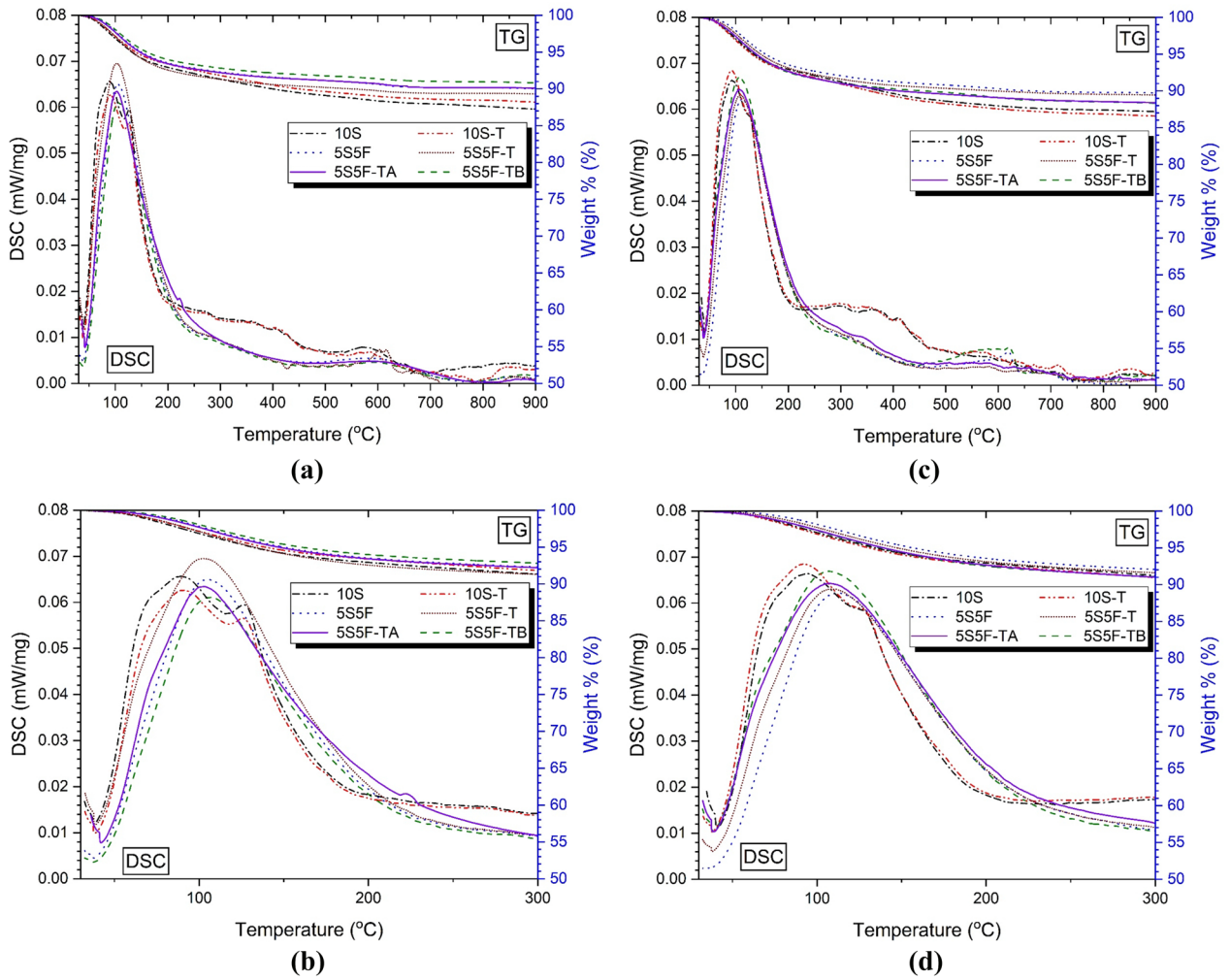

Fig. 5 Thermal analysis (DSC) of samples at 1 day and 28 days, **a** 1 day, **b** enlarge the area smaller than 300°, **c** 28 days, **d** enlarge the area smaller than 300°.

samples with and without SF. Calcite was also observed in the 600–700 °C region (Jeon et al. 2015; Vassileva and Vassilev 2005). In particular, 10S and 10S-T samples composed of 100% slag were able to observe weight loss due to hydrotalcite-like phase at 330–400 °C (Haha et al. 2011; Wang and Scrivender 1995) and monosulfate and

130–200 °C (Mindess et al. 2003). The monosulfate and hydrotalcite-like phases are also observed in the XRD results of 10S and 10S-T methods in Fig. 3. However, in the SF mixed samples, weight loss of monosulfate and hydrotalcite-like phase did not appear. Monosulfate and hydrotalcite-like phases were not observed in the XRD results of Fig. 3 of the SF mixed samples.

In Fig. 5b, 10S and 10S-T methods show high weight loss. This is because 100% slag forms a large amount of hydration products by the activator. Conversely, samples from 5S5F to 5S5F-TB method consist of 50% slag + 50% SF. Therefore, the weight reduction rate is also small because the amount of hydration products is decreased due to activation of slag. However, 5S5F-TB method has the highest weight loss rate. This is attributed to the fact that the hydration action of slag was accelerated by the alkaline environment which was high in the mixing condition. The 5S5F-TB method uses a high-pH alkali activator for total activator + half mixing-water in the 1st-cycle stage. In addition, since only the slag is mixed in the 1st-cycle, the hydration of the slag is rapidly promoted and a large amount of hydration products are formed. Therefore, the weight loss in the DSC is also the highest.

Figure 5d shows weight loss at temperatures less than 300 °C at 28 days. 10S and 10S-T methods still exhibit high weight loss rates. However, unlike in 1 day, 5S5F-TB method showed similar weight reduction rate as 10S-T method. The effect of promoting the formation of hydration products by 5S5F-TB method appears to be highly effective at the initial hydration stage. The weight loss rates at 1 day and 28 days of slag and SF mixed samples were in the order of 5S5F-TB > 5S5F-TA > 5S5F-T > 5S5F. Increasing the mixing time (2nd-cycle) at 10S and 5S5F method accelerated the formation of hydration products. It can be seen from the DSC analysis that the 10S-T and 5S5F-T methods samples show higher weight loss rates than 10S and 5S5F methods.

Thermal analysis showed that the hydration action of slag influenced the weight loss. This clearly shows the difference in weight loss in the method of mixing slag first at 100% slag or 1st-cycle. In particular, when comparing 5S5F-TA and 5S5F-TB method, 5S5F-TB with half the mixing-water shows a higher weight loss rate. This is due to the formation of a relatively higher aqueous alkali solution in the 1st-cycle, thereby promoting the hydration of slag. Therefore, the difference in mixing method affects the formation of hydration reactants depending on whether the activation of slag is accelerated at an early stage.

3.5 Ultrasonic Pulse Velocity

Figure 6 shows the results of ultrasonic pulse velocity (UPV) measurements. UPV has been widely used as a method of measuring physical properties such as elastic modulus and compressive strength of concrete (Demirboğa et al. 2004; Omer et al. 2015; Mohammed and Rahman 2016). Reductions in UPV values indicate material deterioration, internal cracks, and/or pre-existing defects that may occur in the paste (Omer et al. 2015). Therefore, it can be concluded that the increase of UPV is due to the formation of dense matrix with few pores, cracks and defects.

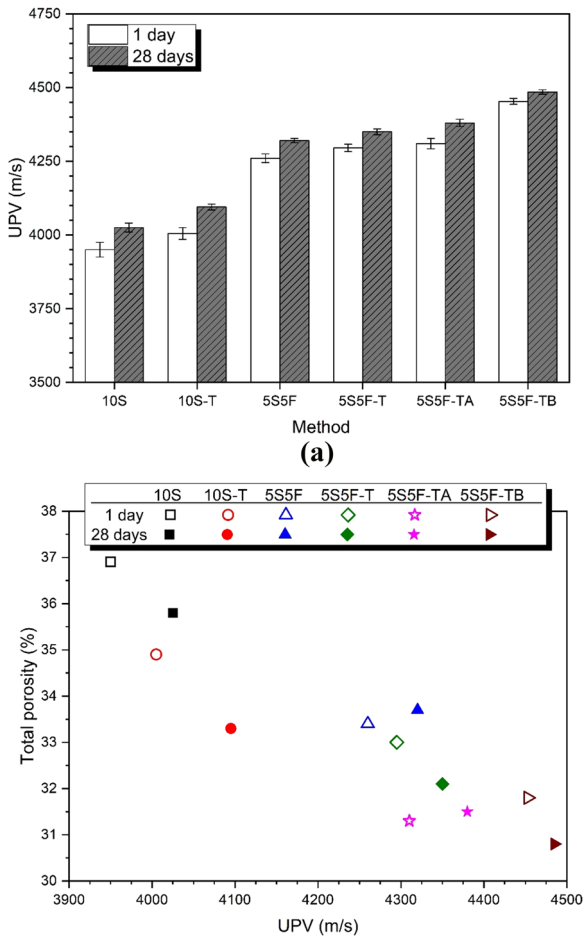

Fig. 6 Ultrasonic pulse velocity and total porosity **a** ultrasonic pulse velocity, **b** ultrasonic pulse velocity vs total porosity.

Therefore, the correlation between the strength characteristics of the specimen and the mixing method was investigated through UPV measurement. In all samples, UPV of 28 days was more than 1 day. Also, the UPV of 50% slag + 50% SF samples was larger than that of 100% slag 10S/10S-T. The increase in UPV means that the sample is dense without pores, cracks, and foreign matter. Therefore, the substitution of SF has the effect of forming dense hydration products (Uysal et al. 2018). As a result,

the total porosity decreases and the compressive strength increases. 10S-T and 5S5F-T method show increased UPV over 10S and 5S5F-T methods. This is because the addition of the mixing time by the 2nd-cycle increases the UPV by forming a dense matrix.

The UPV of 5S5F-TA method was slightly higher than that of 5S5F-T method. The highest UPV was 5S5F-TB method. This is similar to the results shown in the compressive strength and pore structure previously described. The highest compressive strength and lowest total porosity were 5S5F-TB method. Figure 6b shows the relationship between UPV and total porosity. As the total porosity decreases, the UPV increases.

Therefore, adjustment of the mixing method will be sufficient to increase the formation of hydration products and to form a more dense matrix.

3.6 Microstructural Analysis

In Fig. 2 and Table 4, the compressive strength values at 1 day, 7 days, and 28 days were compared with the values of 5S5F-T, 5S5F-TA, and 5S5F-TB for 5S5F. 5S5F-T had the highest 1 day compressive strength increase rate of 116.6%, the highest compared to 108.8% of 7 days and 105.5% of 28 days. 5S5F-TA showed compressive strength increase rate of 114.9% at 1 day, similar to 115.0% of 7 days, but higher than 109.9% of 28 days. The difference between the compressive strength increase rate of 1 day and 7 days of 5S5F-TA was only 0.1%. The compressive strength increase rate of 5S5F-TB was 133.0% at 1 day, and this value was higher than 126.5% at 7 days and 127.2% at 28 days. As mentioned in the results as described above, 5S5F-T, 5S5F-TA, and 5S5F-TB had a high rate of increase in compressive strength at 1 day. In the case of 5S5F-TA, the compressive strength increase rate of 1 day and 7 days was similar with 0.1% difference. However, 5S5F-T and 5S5F-TB clearly showed the largest increase rate at 1 day. As a result, 5S5F-T, 5S5F-TA, and 5S5F-TB can be seen that the difference in mixing method had a greater effect on the rate of increase in strength at 1 day than in other ages. This means that the mixing method has a great influence on the mechanical performance in the early age. Therefore, we will examine the hydration products and matrix of the samples at 1 day.

The hydration products observed in SEM/BSE were similar regardless of mixing method. The difference in the visually confirmed hydration products matrix was not clear (see Fig. 7).

The energy dispersive X-ray spectroscopy (EDS) analysis was carried out to confirm the difference of the hydration products according to the mixing method. In EDS analysis, 5 spots were arbitrarily selected from the hydration products matrix around the unhydrated slag particles in Fig. 8. Figure 8 shows the Ca/Si and Al/Si ratios obtained by EDS analysis. The values of Ca/Si and Al/Si have various values depending on the substitution rate of SF, kind and concentration of activator, curing condition, and the like (Burciaga-Díaz and Escalante-García 2013; Alanazi et al. 2019; Gülşan et al. 2019; Zhang et al. 2020; Aydin 2013; Cheah et al. 2019; Haha et al. 2012).

In Fig. 8, the highest mixing method of Ca/Si was the 5S5F-TB method, followed by the 5S5F-TA method. The 10S-T and 5S5F-T- methods showed higher Ca/Si values than the 10S and 5S5F- methods. This suggests that the Ca/Si value increased as the activation of the slag was promoted and the production of hydration products increased. It can be confirmed that the increase of the mixing time accelerates the hydration of slag as in the method of 10S-T and 5S5F-T methods. It was also confirmed that the formation of a high concentration of alkali aqueous solution in the 1st-cycle like 5S5F-TB method promotes the hydration of slag.

Lower Ca/Si ratios of C-S–H (which is the main reaction product of AASC) correspond to lower C-S–H densities and, hence, to lower strength. This is because the amount of H_2O in C-S–H increases (Hah et al. 2012). The highest compressive strength of 5S5F-TB method (which has the highest Ca/Si ratio) was also measured. 10S, with the lowest Ca/Si ratio, showed the lowest compressive strength. In the OPC-based study, it was reported that as the substitution ratio of SF increases, Ca/Si of C-S–H decreases (Rossen et al. 2015). However, in this study, the composition ratio of slag and SF is constant at 1 : 1. Nevertheless, the change in the mixing method changes the Ca/Si value. This means that the change of the mixing method accelerates hydration of slag and affects Ca/Si value of hydration products.

The highest Al/Si value was 5S5F-TB method. Therefore, the use of a high alkaline aqueous solution for accelerating the hydration of slag in the 1st-cycle is an important factor affecting the formation of hydration products. As a result of EDS analysis of alkali-activated cement hydration products using 100% slag, Al/Si value increased with increasing age. As time goes on, the hydration of the slag also continues slowly and thus the Al/Si value increases (Burciaga-Díaz and Escalante-García 2013). Therefore, when the hydration reaction is promoted by the activation of slag, the Al/Si value increases. The increase of Al/Si can be confirmed by the change of Al/Si value according to the mixing method as shown in Fig. 8. 5S5F-TB method is considered to have increased Al/Si by applying a high-pH alkaline aqueous solution that promotes hydration of slag in the 1st-cycle.

The results of the OPC-based, slag-based alkali-activated cement, and fly ash-based geopolymer considered

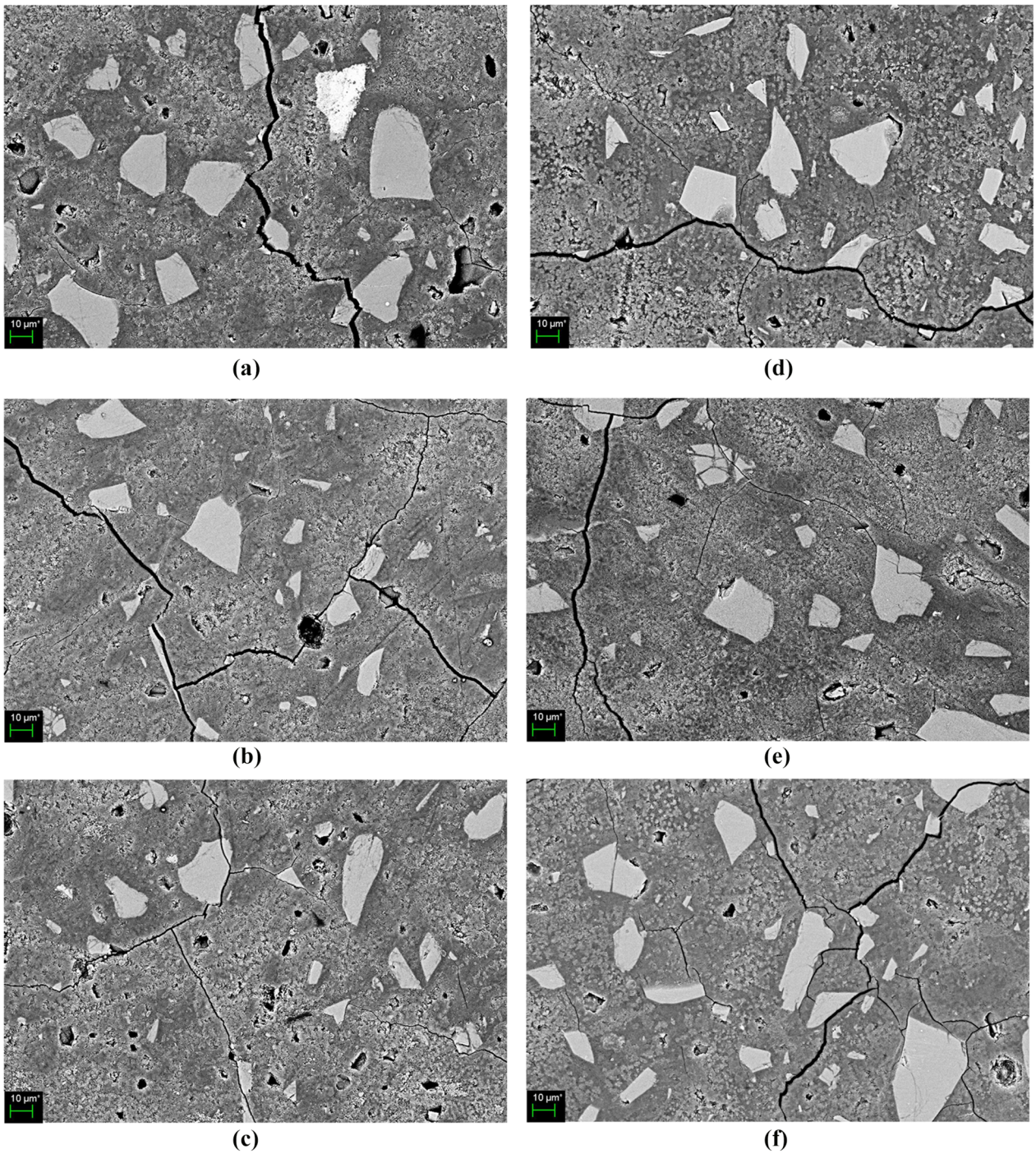

Fig. 7 SEM/BSE images at 1 day **a** 10S, **b** 10S-T, **c** 5S5F, **d** 5S5F-T, **e** 5S5F-TA, **f** 5S5F-TB.

in the previous studies refer to the formation of C-S–H gel and the change of Ca/Si and Al/Si values according to the substitution ratio of SF. It is difficult to make a clear comparison with the results of the previous studies because there is almost no comparative analysis of the hydration products according to the composition ratio and mixing method of the constant slag-SF considered in this study. However, it is clear that changes in mixing methods affect the formation and composition of hydration products.

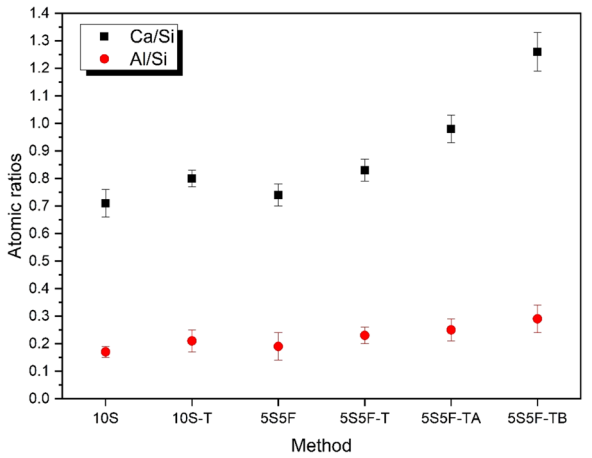

Fig. 8 Atomic ratios of hydration products.

4 Conclusion

The results of the investigation on the characteristics of the alkali-activated cement paste for the binder composed of slag and silica fume (SF) of 1: 1 are summarized as follows.

- Increasing the mixing time promotes hydration due to the uniform distribution of slag and SF and the increase in the contact area and time of the activator with the slag particles. This action produces dense hydration reactants, reduces total porosity and increases compressive strength. Therefore, it was confirmed that the increase of the mixing time should be considered as a factor affecting the improvement of pore structure and mechanical properties by promoting the activation reaction of slag and increasing the formation of hydration reactants.
- The method of accelerating the slag using the activator of high alkali concentration in the 1st-cycle shows the highest compressive strength and the lowest total porosity. The promotion of slag activation in the early stages of mixing was effective to improve the mechanical properties. Therefore, the method of mixing slag prior to SF in a high alkaline environment by controlling the amount of mixing-water is an important factor in sufficiently improving the mechanical properties.
- Mixing SF in 2nd-cycle is done for slag paste already mixed in 1st-cycle. As a result, it can be estimated that SF is an effective step for homogeneous dispersion in slag paste by applying 2nd-cycle. Therefore, the filler effect and nucleation effect of SF help to show the improved mechanical properties. The effect of this action is demonstrated by 5S5F-TB method showing the highest mechanical performance and low total porosity.

The results of this study confirmed the possibility of improving the mechanical performance just by the change of the mixing method without the increase of the activator concentration, the high temperature curing, and the use of the additional admixture.

Acknowledgements
The authors thank the Core Research Facility of Pusan National University funded by the Korea Ministry of Education for the technical support on XRD and SEM analysis.

Authors' contributions
All authors contributed to the paper. All authors read and approved the final manuscript.

Authors' information
Taewan Kim is a Research Professor at the Department of Civil Engineering at Pusan National University. The major research areas are concrete structures and materials. Current interests are self-healing, ultra-lightweight concrete, eco-firendly cement and UHPC precast concrete construction technology.

Choonghyu Kang is a Assistant Professor in Department of Ocean Civil Engineering at Gyeongsang National University. He is interested in the properties of construction materials, especially concrete materials. He is studying about crack propagation, tension-softening, crack analysis now.

Funding
This work was supported by the National Research Foundation of Korea(NRF) Grant funded by the Korea Government(MOE) (NRF-2015R1D1A3A01019583 and NRF-2017R1D1A1B03034470).

Availability of data and materials
Please contact author for data requests.

Competing interests
The authors declare that they have no competing interests.

Author details
[1] Department of Civil Engineering, Pusan National University, Busan 46241, Republic of Korea. [2] Department of Ocean Civil Engineering, Gyeongsang National University, Tongyeong 53064, Republic of Korea.

Received: 29 January 2020 Accepted: 5 May 2020
Published online: 29 June 2020

References

Alanazi, H., Hu, J., & Kim, Y.-R. (2019). Effect of slag, silica fume, and metakaolin on properties and performance of alkali-activated fly ash cured at ambient temperature. *Construction and Building Materials, 197,* 747–756.
Awoyera, P., & Adesina, A. (2019). A critical review on application of alkali activated slag as a sustainable composite binder. *Case Studies in Construction Materials, 11,* e002668.
Awoyera, P. O., Adesina, A., Sivakrishna, A., Gobinath, R., Rajesh Kumar, K., & Srinivas, A. (2019). Alkali activated binders: Challenges and opportunities. *Materials Today: Proceedings*. https://doi.org/10.1016/j.matpr.2019.08.199.
Aydin, S. (2013). A ternary optimisation of mineral additives of alkali activated cement mortars. *Construction and Building Materials, 43,* 131–138.
Aydın, S., & Baradan, B. (2013). The effect of fiber properties on high performance alkali-activated slag/silica fume mortars. *Composites: Part B, 45,* 63–69.
Bakolas, A., Aggelakopoulou, E., Moropoulou, A., & Anagnostopoulou, S. (2006). Evaluation of pozzolanic activity and physicomechanical characteristics

in metakaolin-lime pastes. *Journal of Thermal Analysis and Calorimetry, 84,* 157–163.
Behfarnia, K., & Rostami, M. (2017). Effects of micro and nanoparticles of SiO_2 on the permeability of alkali activated slag concrete. *Construction and Building Materials, 131,* 205–213.
Bernal, S. A., & Provis, J. L. (2014). Durability of alkali-activated materials: Progress and perspectives. *Journal of American Ceramic Society, 97,* 997–1008.
Berodier, E., & Scrivener, K. (2014). Understanding the filler effect on the uncleation and growth of C-S–H. *Journal of American Ceramic Society, 94,* 3764–3773.
Burciaga-Díaz, O., & Escalante-García, J. I. (2013). Structure, Mechanisms of reaction, and strength of an alkali-activated blast-furnace slag. *Journal of American Ceramic Society, 96,* 3939–3948.
Cheah, C. B., Tan, L. E., & Ramli, M. (2019). The engineering properties and microstructure of sodium carbonate activated fly ash/slag blended mortars with silica fume. *Composites: Part B, 160,* 558–572.
Collins, F., & Sanjayan, J. G. (1999). Effects of ultra-fine materials on workability and strength of concrete containing alkali-activated slag as the binder. *Cement and Concrete Research, 29,* 459–462.
Demirboğa, R., Türkmen, İ., & Karakoç, M. B. (2004). Relationship between ultrasonic velocity and compressive strength for high-volume mineral-admixtured concrete. *Cement and Concrete Research, 34,* 2329–2336.
Diamond, S., & Sahu, S. (2006). Densified silica fume: particle size and dispersion in concrete. *Materials and Structures, 39,* 849–859.
Duan, P., Shui, Z., Chen, W., & Shen, C. (2013). Effects of metakaolin, silica fume and slag on pore structure, interfacial transition zone and compressive strength of concrete. *Construction and Building Materials, 44,* 1–6.
Gao, X., Yu, Q. L., & Brouwers, H. J. H. (2015). Characterization of alkali activated slag-fly ash blends containing nano-silica. *Construction and Building Materials, 98,* 397–406.
Gülşan, M. E., Alzeebaree, R., Rasheed, A. A., Niş, A., & Kurtoğlu, A. E. (2019). Development of fly ash/slag based self-compacting geopolymer concrete using nano-silica and steel fiber. *Construction and Building Materials, 211,* 271–283.
Haha, M. B., Le Saout, G., Winnefeld, F., & Lothenbach, B. (2011). Influence of activator type on hydration kinetics, hydrate assemblage and microstructural development of alkali activated blast-furnace slags. *Cement and Concrete Research, 41,* 301–310.
Haha, M. N., Lothenbach, B., Le Saout, G., & Winnefeld, F. (2012). Influence of slag chemistry on the hydration of alkali-activated blast-furnace slag—Part II: Effect of Al_2O_3. *Cement and Concrete Research, 42,* 74–83.
Jeon, D., Jun, Y., Jeong, Y., & Oh, J. E. (2015). Microstructural and strength improvements through the use of Na_2CO_3 in a cementless $Ca(OH)_2$-activated Class F fly ash system. *Cement and Concrete Research, 67,* 215–225.
Li, Z., Pan, Z., Liu, Y., He, L., Duan, W., Collins, F., et al. (2014). Effects of mineral admixtures and lime on disintegration of alkali-activated slag exposed to 50 °C. *Construction and Building Materials, 70,* 254–261.
Mindess, S., Young, J. F., & Darwin, D. (2003). *Concrete* (2nd ed.). Upper Saddle River: Prentice Hall.
Mohammed, T. U., & Rahman, M. N. (2016). Effect of types of aggregate and sand-to-aggregate volume ratio on UPV in concrete. *Construction and Building Materials, 125,* 832–841.
Nochaiya, T., Wongkeo, W., & Chaipanich, A. (2010). Utilization of fly ash with silica fume and properties of Portland cement-fly ash-silica fume concrete. *Fuel, 89,* 768–774.
Omer, S. A., Demirboga, R., & Khushefati, W. H. (2015). Relationship between compressive strength and UPV of GGBFS based geopolymer mortars exposed to elevated temperatures. *Construction and Building Materials, 94,* 189–195.
Palacios, M., & Puertas, F. (2011). Effectiveness of mixing time on hardened properties of waterglass-activated slag pastes and mortars. *ACI Materials Journal, 108*(1), 73–78.
Provis, J. L., Palomo, A., & Shi, C. (2015). Advances in understanding alkali-activated materials. *Cement and Concrete Research, 78,* 110–125.
Ramezanianpour, A. A., & Moeini, M. A. (2018). Mechanical and durability properties of alkali activated slag coating mortars containing nanosilica and silica fume. *Construction and Building Materials, 163,* 611–621.
Rashad, A. M. (2013). A comprehensive overview about the influence of different additives on the properties of alkali-activated slag—A guide for civil engineer. *Construction and Building Materials, 47,* 29–55.
Rashad, A. M., & Khalil, M. H. (2013). A preliminary study of alkali-activated slag blended with silica fume under the effect of thermal loads and thermal shock cycles. *Construction and Building Materials, 40,* 522–532.
Rossen, J. E., Lothenbach, B., & Scrivener, K. L. (2015). Composition of C-S–H in pastes with increasing levels of silica fume addition. *Cement and Concrete Research, 75,* 14–22.
Rostami, M., & Behafarnia, K. (2017). The effect of silica fume on durability of alkali activated slag concrete. *Construction and Building Materials, 134,* 262–268.
Sun, J., Zhang, Z., Zhuang, S., & Hw, W. (2020). Hydration properties and microstructure characteristics of alkali–activated steel slag. *Construction and Building Materials, e241,* 118141.
Uysal, M., Al-mashhadani, M. M., Aygörmez, Y., & Canpolat, O. (2018). Effect of using colemanite waste and silica fume as partial replacement on the performance of metakaolin-based geopolymer mortars. *Construction and Building Materials, 176,* 271–282.
Vassileva, C. G., & Vassilev, S. V. (2005). Behaviour of inorganic matter during heating of Bulgarian coals: 1. *Lignites. Fuel Processing Technology, 86,* 1297–1333.
Wang, S. D., & Scrivener, K. L. (1995). Hydration products of alkali activated slag cement. *Cement and Concrete Research, 25,* 561–571.
Wetzal, A., & Mddendorf, B. (2019). Influence of silica fume on properties of fresh and hardened ultra-high performance concrete based on alkali-activated slag. *Cement & Concrete Composites, 100,* 53–59.
Wongkeo, W., Thongsanitgarn, P., & Chaipanich, A. (2012). Compressive strength and drying shrinkage of fly ash-bottom ash-silica fume multi-blended cement mortars. *Materials and Design, 36,* 655–662.
Zhang, Q., Ji, T., Yang, Z., Wang, C., & Wu, H. (2020). Influence of different activators on microstructure and strength of alkali-activated nickel slag cementitious materials. *Construction and Building Materials, 235,* 117449.
Zhang, M. H., & Li, H. (2011). Pore structure and chloride permeability of concrete containing nano-particles for pavement. *Construction and Building Materials, 25,* 608–616.

Publisher's Note

Springer Nature remains neutral with regard to jurisdictional claims in published maps and institutional affiliations.